NANO LETTERS

2008
Vol. 8, No. 8
2336-2340

Atomistic Mechanisms of ZnO Aggregation from Ethanolic Solution: Ion Association, Proton Transfer, and Self-Organization

Agnieszka Kawska, Patrick Duchstein, Oliver Hochrein, and Dirk Zahn*

Max-Planck Institut für Chemische Physik fester Stoffe, Nöthnitzerstr. 40, D-01187 Dresden, Germany

Received April 25, 2008; Revised Manuscript Received June 5, 2008

ABSTRACT

We report on atomistic simulations related to the nucleation of zinc oxide nanocrystals from ethanolic solution. The underlying mechanisms are explored from the very initial stage of Zn^{2+} and OH^- ion association to the formation of nanometer-sized aggregates counting up to 250 ions. The embryonic aggregates consist of zinc and hydroxide ions, only. At later stages of aggregate growth, proton transfer reactions at the aggregate−solvent interface account for the formation of O^{2-} ions and induce the precipitation of zinc oxide. After the association of around 150 ions, ZnO domains were found to nucleate in the central region of the $[Zn_x(OH)_yO_z]^{2x-y-2z}$ aggregates. In the course of further ion association and condensation reactions, progressive self-organization leads to an extended core in which the ions are arranged according to the wurtzite structure.

Apart from its wide use for UV protection, nanocrystals of zinc oxide exhibit a large variety of interesting potential applications including room temperature UV lasers,[1] LEDs,[2] solar cells,[3] and sensors.[4] Moreover, they also represent a protype model for the exploration of oxide nanocrystal precipitation from solution. Most of the related sol−gel processes are based on alcoholic solutions of Zn^{2+} and OH^- ions (plus counterions originating to the reactant materials).[5,6] Nevertheless, stable $Zn(OH)_2$ crystals are typically not observed.[7] Instead, the most common precipitation reactions involve proton transfer leading to the formation of oxide ions and the crystallization of ZnO. The key to the understanding of ionic self-organization from solution and its interplay with ion−solvent interactions originates to the atomistic scale. For such investigations,in particular when related to the very early stage of ion association and crystal nucleation from solution, advanced molecular simulation techniques proved to be a promising tool and considerably extended our mechanistic understanding.[8–10]

One of these approaches is represented by our recently developed simulation scheme for aggregate growth from solution[10] which is divided in subsequent steps as illustrated in Scheme 1. In each iteration, single ions are added to an aggregate which is then subjected to relaxation processes, including proton transfer reactions. Choosing a single ion as the initial aggregate allows the investigation of ion association and self-organization from its very beginning.

For each aggregate growth attempt, the first step (i) is given by a docking-like approach for searching putative sites for ion association. The ionic species is chosen randomly as Zn^{2+} or OH^- ions (imposing a 1:2 ratio). To mimic the effect of ion migration from solution, the incoming ion is placed on the surface of a sphere which envelops the aggregate. In keeping the ionic positions of the central aggregate fixed, the solvent molecules are removed, and a putative site for ion association is identified from steepest descend minimization of the interactions of the aggregate and the incoming ion. In the next steps (ii and iii), the solvent is reintroduced. Subsequent relaxation by simulated annealing is first applied to the solvent molecules only (ii) and then to the whole system (iii).[10]

Steps i−iii are modeled by means of empirical force-fields and do not require quantum calculations. However, as an extension to the original aggregate growth scheme[10] the resulting configuration of step iii is scanned for hydrogen bonds which might induce proton transfer reactions. In the new iteration step (iv) the H···O distances of the hydrogen bonds interconnecting the OH^- ions are calculated, and the shortest hydrogen bond is taken as a candidate for proton transfer. The putative reaction $A-OH^-\cdots OH^- \rightarrow A-O^{2-} + H_2O$ (A = aggregate) is then explored from combined quantum/classical molecular mechanics calculations. For the

* Corresponding author. E-mail: zahn@cpfs.mpg.de. Phone: (+49) 351-46463001. Fax:(+49) 351-46463002.

10.1021/nl801169x CCC: $40.75
Published on Web 06/24/2008

Scheme 1. Simulation Scheme for Aggregate Growth

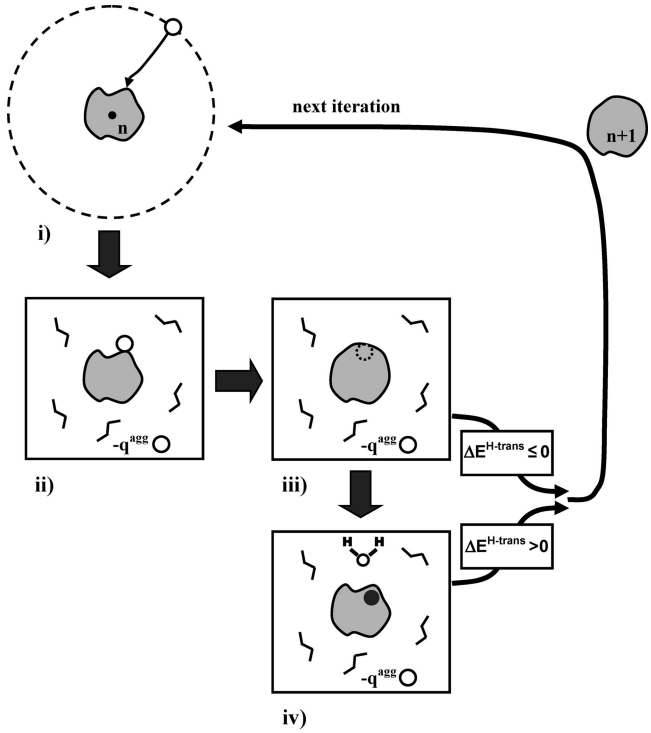

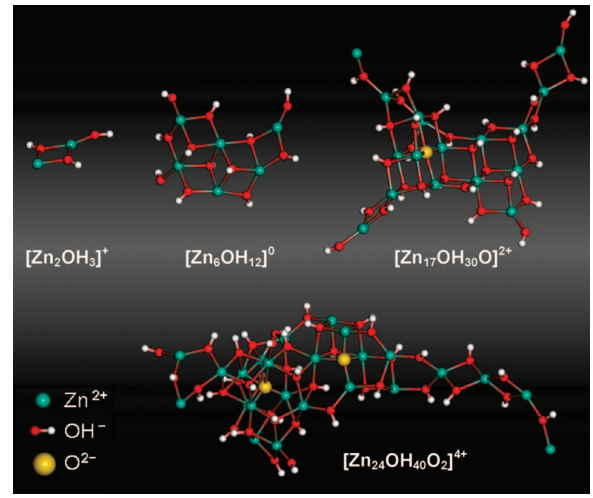

Figure 1. Snapshots of the early stage of aggregate formation (solvent molecules are not shown). Aggregates counting only a few tens of ions comprised of Zn^{2+} and OH^- ions, only. Self-organization of these ions leads to motifs exhibiting similarities to the rocksalt structure. At later stages of the aggregate growth, O^{2-} ions result from proton transfer reactions (see also Figure 2). This process is accompanied by dramatic structural rearrangements.

sake of computational feasibility (the possibility of proton transfer is explored after every ion association event), we only compute the energy levels of the reactant and the product state. This covers the essential aspect of the putative reaction, that is, whether proton transfer is exothermic or not. Both possible states are relaxed from simulated annealing before the energetically more favorable constellation is taken as the starting point for the next aggregate growth event.

$$\Delta E^{H^+-transfer} = E^{qm}_{vacuum}(O^{2-} + H_2O) - E^{qm}_{vacuum}(OH^- + OH^-) - \{E^{cl}_{vacuum}(O^{2-} + H_2O) - E^{cl}_{vacuum}(OH^- + OH^-)\} + E^{cl}_{solvent}([Zn_x(OH)_{y-2}O_{z+1}]^{2x-y-2z} + H_2O) - E^{cl}_{solvent}([Zn_x(OH)_yO_z]^{2x-y-2z}) \quad (1)$$

Hamiltonian of the Quantum/Classical (qm/cl) Calculations. The first terms originate to the quantum calculation of the reacting subsystem in vacuum. From this, the corresponding energy levels of the classical force-field description is subtracted (second line) to avoid double counting in the classical modeling of the ion−ion interactions. The last two terms reflect the ion−ion and ion−solvent interactions of the aggregate before and after proton transfer, respectively. During relaxation of the putative product state (involving the formation of O^{2-} and H_2O), the water molecule was always found to migrate to the ethanolic solution. In the vacuum calculations related to the product state, the distances of the O^{2-} ion and the water molecule were therefore taken as infinite.

The quantum calculations of the electronic ground states were performed using the Gaussian package at the 6−311** basis set and second order Moller−Plesset perturbation theory for considering electron correlation. For the classical molecular mechanics simulations, empirical force fields[11–13] were taken from the literature as described in detail in Supporting Information. To mimic a bulk ethanolic solution, the aggregate is placed in a cubic box (~4 × 4 × 4 nm^3) of 750 ethanol molecules. Periodic boundary conditions are applied, and temperature and pressure are constrained to 300 K and 1 atm, respectively. For the molecular dynamics simulations, a time-step of 1 fs was found to be appropriate. For each aggregate growth iteration, the relaxation process following the association of the newly added ion amounts to a simulation time of 100 ps (see ref 10 for more details). The following analysis is based on three independent growth runs. While the illustrations show representative configurations of a single growth run, the presented statistics correspond to the data from all simulations runs.

The very initial stage of the aggregation process corresponds to the association of Zn^{2+} and OH^- ions from the ethanolic solution. Strikingly, self-organization may already be observed in aggregates counting less than 20 ions (Figure 1). In this premature ordering, the zinc ions are coordinated by OH^- ions arranged as (incomplete) octahedra similar to the rocksalt structure. In this constellation, the hydrogen atoms of the OH^- groups points to the solvent and $H^{\delta+}\cdots Zn^{2+}$ contacts are avoided. Consequently, the formation of extended domains of such motifs is clearly hindered. Indeed, the preordering represents a very temporary feature which changes dramatically in the course of local O^{2-} ion formation as discussed in the following.

At the aggregate surface, the hydroxide ions predominantly form hydrogen bonds with the ethanolic solution. However, in the course of further OH^- ion association temporary $OH^-\cdots OH^-$ interconnections leading to proton transfer reactions are observed. Figure 2 shows the first proton transfer event observed from one of our aggregate growth simulations. A newly associated hydroxide ion experiences electrostatic bonding to two Zn^{2+} ions and hydrogen bonding to

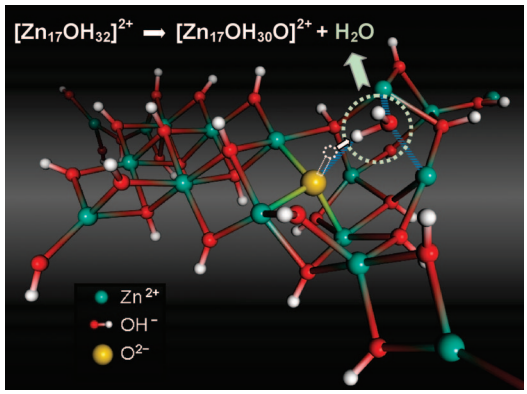

Figure 2. Onset of ZnO formation by condensation reactions. At the aggregate surface, a newly associated hydroxide ion (top right) experiences hydrogen bonding to the hydrogen atom of an adjacent OH^- ion. This hydrogen bond is used for exothermic proton transfer. The resulting water molecule migrates into the solvent, whereas the O^{2-} ion remains within the aggregate.

the hydrogen atom of a neighboring OH^- ion. Along this hydrogen bond, proton transfer was found to be exothermic. The resulting H_2O molecule is only loosely affiliated to the aggregate and eventually diffuses into the ethanolic solution. On the other hand, the O^{2-} ion remains in the aggregate and gives rise to dramatic structural rearrangements.

A first insight into the effect of O^{2-} ion formation on the relaxation of the aggregate may be obtained from the $[Zn_{24}(OH)_{40}O_2]^{4+}$ agglomerate illustrated in Figure 1 (bottom). Already after the formation of only two O^{2-} ions, the earlier observed preordering (octahedral coordination) of the aggregate is rearranged in favor of the wurtzite structure (tetrahedral coordination). Further aggregate growth leads to a systematically increasing dominance of oxide ions. Though the hydroxide ions represent the major anionic species at the aggregate surface, agglomerates counting more than around 150 ions exhibit a core which is fully sparse of OH^-. The ionic arrangement in this core region may be described by six-membered rings, formed as either chair- or boat-type constellations. The automated identification of these motifs is based on a geometric hashing algorithm as described in Supporting Information.

Figure 3a illustrates the beginning of ZnO ordering in the aggregate center. At this stage of aggregate growth, most of the six-ring motifs are randomly oriented (see Figure 4 for the total number of chair and boat motifs as a function of aggregate size). However, the two highlighted chair-type motifs exhibit a staggered arrangement and represent the onset of orientation correlation between the six rings. Indeed, the staggered arrangement does not undergo substantial changes during further crystal growth and is hence suggested as a center of stability. This assumption is supported by the observation of progressive ordering in the same manner starting from this nucleus. Figure 3b shows the aggregate after the uptake of about 50 more ions. Adjacent to the staggered six-ring motifs highlighted in Figure 3a, further chair motifs of matching orientation were formed. The ionic ordering of the ZnO nanocrystal hence nucleates in the center

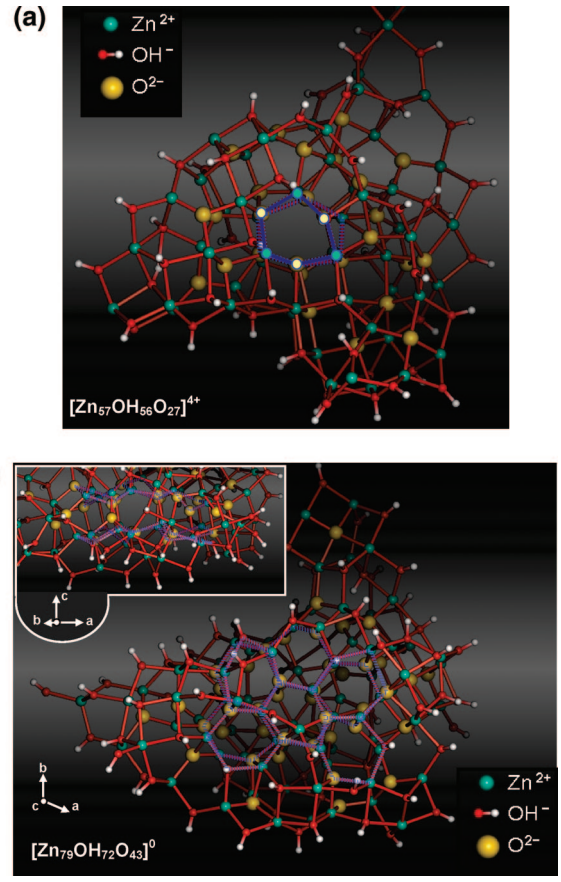

Figure 3. Nucleation and growth of domains of the wurtzite structure. The characteristic six rings are highlighted in blue and discussed more quantitatively in Figure 4. (a) Self-organization of the ZnO crystal structure is initiated in the aggregate center which contains no OH^- ions. The two staggered six ring form a center of stability and give rise to further ordering in favor of the wurtzite structure. The upper six ring is highlighted for better visibility. (b) At later stages of aggregate growth, progressive self-organization results in the formation of an extended core comprising of Zn^{2+} and O^{2-} ions ordered in chair and boat motifs corresponding to the wurtzite structure. For better visibility, only chair-type six-ring motifs are highlighted.

of the agglomerates and, in the course of further aggregate growth, propagates within the increasing bulk domain.

In the hexagonal wurtzite structure, the ABAB stacking of layers of Zn−O six ring along the *c* axis gives rise to boat motifs connecting adjacent (001) layers (Figure 4, top right). This feature helps to discriminate the ionic arrangement from the cubic sphalerite structure. In sphalerite, the individual (001) layers are identical to those of the wurtzite structure but stacked in terms of ABCABC. As a consequence, neighboring (001) layers are connected by chair rather than boat motifs. We performed an analysis of the number of chair and boat motifs as a function of the aggregate size (Figure 4). Despite the small numbers of ions available, self-organization already causes chair and boat motif formation roughly at the 1:3 ratio present in the ideal wurtzite structure. To illustrate the resulting stacking of layers, a close up of the ordered core of the $[Zn_{79}(OH)_{72}O_{43}]$ aggregate is also shown at different orientation in the top left of Figure 3b.

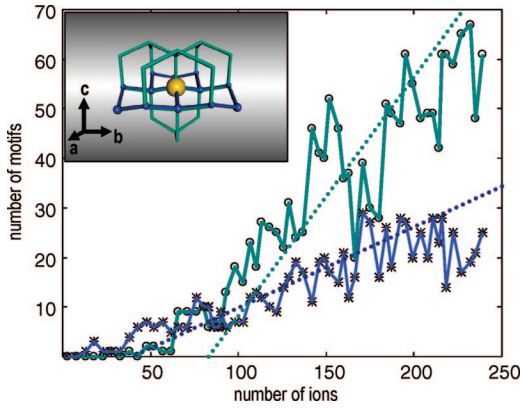

Figure 4. Number of chair (blue) and boat (green) motifs as a function of the aggregate size. The slopes of the dotted lines indicate chair and boat motif formation at a ratio of 1:3 as corresponding to the ideal wurtzite structure. The later is illustrated by the inset in the top left which depicts the 3 chair and 9 boat motifs coordinating each ion (yellow).

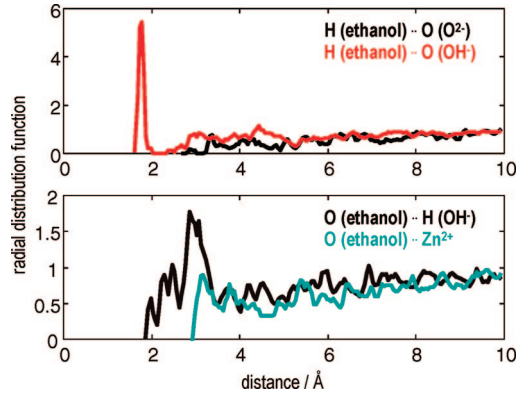

Figure 5. Radial distribution functions of the solvent−ion distances as obtained for the aggregate depicted in Figure 3b. Anion−solvent interactions are only observed for OH^- ions; the O^{2-} ions are located in the inner core of the aggregate.

A geometric analysis of the Zn−O six rings may be given by the interionic distances and angles. In the aggregate core, the nearest neighbor Zn^{2+}···O^{2-} distance was found to vary from 1.8 to 2.1 Å, whereas the Zn^{2+}···OH^- distances range from 2.0 to 2.2 Å. From crystal structure refinements of bulk ZnO, the corresponding distances were found as 1.9746(1) Å (basal) and 1.9857(1) Å (apical), respectively.[14] Moreover, the Zn−O−Zn/O−Zn−O angles of neighboring ion triples in the aggregate center were found to range from 100 to 120° which also is in reasonable agreement with experiments related to the bulk material (108.11(2) and 110.79(2)°, respectively). Detailed statistics are provided in Supporting Information.

At the aggregate−solvent interface, ionic ordering is much less pronounced compared with the nanocrystal core. However, a typical feature of the aggregate−solvent interface is given by the vanishing occurrence of O^{2-} species and the dominance of OH^- ions which hydrogen atom points toward the ethanolic solvent. Figure 5 depicts radial distribution functions calculated for the solvent−ion distances of the $[Zn_{79}(OH)_{72}O_{43}]$ aggregate shown in Figure 3. The upper plot refers to hydrogen bonding of the OH group of ethanol to the anions of the nanocrystal. Ethanol−oxide ion hydrogen bonds are only rarely observed. The O^{2-} ions are thus separated from the solvent and occur only in the inner part of the nanocrystal. Scanning the whole series of aggregates obtained from our calculations, we found at most one single oxide ion at the interface to the solvent. The OH^- ions are hence the dominating anionic species at the aggregate surface. In average, the hydroxide ion−solvent interactions involve one to two H(ethanol)···O(OH^-) and at most one O(ethanol)···H(OH^-) hydrogen bond. On the other hand, the Zn^{2+} ions of the aggregate surface form 1−2 electrostatic bonds to the oxygen atoms of the ethanol molecules.

As part of our modeling approximations, the ethanolic solution embedding the aggregates is taken to be free of further ions. While the dissociation of water and Zn^{2+}/OH^- ions from the aggregate are considered during the relaxation runs, a quantitative assessment of the interplay of ion uptake/dissociation exceeds the scope of the present work. The different chemical potentials of the ionic species depend on the respective concentration in the solution and so does the size of the critical nucleus. However, from our work, two important aspects of aggregate stabilization can be identified: (i) ripening reactions leading to the formation of O^{2-} ions and (ii) nucleation and growth of a ZnO domain of wurtzite crystal structure type.

In conclusion, we elucidated the atomistic mechanisms of the aggregation of (wurtzite-type) zinc oxide nanocrystals from ethanolic solution. The very initial stage of this process is given by Zn^{2+} and OH^- ions association and the formation of $[Zn_xOH_y]^{2x-y}$ agglomerates exhibiting octahedral coordination constellations. These aggregates of less than 50 ions correspond to precursors which undergo A−OH^-···OH^- → A−O^{2-} + H_2O (A = aggregate) proton transfer reactions. While the resulting water molecule migrates into the solution, the formation of O^{2-} ions implies dramatic changes within the aggregate. Premature ordering is largely reversed, and after the association of around 150 ions, wurtzite-type (tetrahedral coordination constellations) ZnO domains were found to nucleate in the central region of the nanocrystal. While the aggregate surface mainly consists of Zn^{2+} and OH^- ions, the core comprises Zn^{2+} and O^{2-} ions, only. The latter are ordered in Zn−O six rings according to chair and boat motifs which undergo self-organization in favor of the final crystal structure. Aggregates counting more than 200 ions already exhibit a nanometer-sized core of the wurtzite structure which grows in the course of further ion association and condensation reactions.

Acknowledgment. The authors wish to thank Rüdiger Kniep and Stefan Kaskel for very fruitful discussions. The ZIH Dresden is gratefully acknowledged for providing high-performance computing resources.

Supporting Information Available: Geometric hashing of chair and boat motifs, occurrence profiles, empirical interaction potentials and corresponding parameters. This material is available free of charge via the Internet at http://pubs.acs.org.

References

(1) Huang, M. H.; Mao, S.; Feick, H.; Yan, H.; Wu, Y.; Kind, H.; Webber, E.; Russo, R.; Yang, P. *Science* **2001**, *292*, 1897.
(2) Park, W. I.; Yi, G. C.; Kim, J. W.; Park, S. M. *Appl. Phys. Lett.* **2003**, *82*, 4358.
(3) Rensmo, H.; Keis, K.; Lindstrom, H.; Soderen, S.; Solbrand, A.; Hagfeldt, A.; Lindquist, S. E.; Wang, L. N.; Muhammed, M. *J. Phys. Chem. B* **1997**, *101*, 2598.
(4) Kind, H.; Yan, H.; Messer, B.; Law, M.; Yang, P. *Adv. Mater.* **2002**, *14*, 158.
(5) Spanhel, L.; Anderson, M. A. *J. Am. Chem. Soc.* **1991**, *113*, 2826.
(6) Meulenkamp, E. A. *J. Phys. Chem. B* **1998**, *102*, 5566.
(7) Stahl, R.; Jung, C.; Lutz, H. D.; Kockelmann, W.; Jacobs, H. *Z. Anorg. Allg. Chem.* **1998**, *624*, 1130.
(8) Anwar, J.; Boateng, P. K. *J. Am. Chem. Soc.* **1998**, *120*, 9600.
(9) Zahn, D. *Phys. Rev. Lett.* **2004**, *92*, 40801.
(10) Kawska, A.; Brickmann, J.; Kniep, R.; Hochrein, O.; Zahn, D. *J. Chem. Phys.* **2006**, *124*, 24513.
(11) Lewis, G. V.; Catlow, C. R. A. *J. Phys. C: Solid State Phys.* **1985**, *18*, 1149.
(12) Mayo, S. L.; Olafson, B. D.; Goddard, W. A., III *J. Phys. Chem.* **1990**, *94*, 8897.
(13) Jorgensen, W. L. *J. Am. Chem. Soc.* **1996**, *118*, 11225.
(14) Albertsson, J.; Abrahams, S. C.; Kvick, A. *Acta Crystallogr.* **1989**, *B45*, 34.

NL801169X